Received: 4 March 2024 | Revised: 18 May 2024 | Accepted: 25 May 2024

DOI: 10.1002/ame2.12449

ORIGINAL ARTICLE

Establishment of a humanized ST6GAL1 mouse model for influenza research

Lyu Chao[1] | Han Feng[2] | Gao Qian[3] | Lv Limin[2] | Lu Ziwei[1] | Lu Shuangshuang[1] | Li Xiaoyan[1] | Hu Yuechao[3] | Yang Mengjie[3,4] | Zhao Yingze[3] | Liu Jun[3] | Lu Xuancheng[1] | Duo Shuguang[2]

[1]National Key Laboratory of Intelligent Tracking and Forecasting for Infectious Diseases, Chinese Center for Disease Control and Prevention, Beijing, China

[2]Institute of Zoology, Chinese Academy of Sciences, Beijing, China

[3]NHC Key Laboratory of Biosafety, National Key Laboratory of Intelligent Tracking and Forecasting for Infectious Diseases, National Institute for Viral Disease Control and Prevention, Chinese Center for Disease Control and Prevention, Beijing, China

[4]Zhejiang Provincial Key Laboratory of Medical Genetics, Key Laboratory of Laboratory Medicine, Ministry of Education, School of Laboratory Medicine and Life Sciences, Wenzhou Medical University, Wenzhou, China

Correspondence
Lu Xuancheng, National Key Laboratory of Intelligent Tracking and Forecasting for Infectious Diseases, Chinese Center for Disease Control and Prevention, Beijing, China.
Email: luxc@chinacdc.cn

Duo Shuguang, Institute of Zoology, Chinese Academy of Sciences, Beijing, China.
Email: duoshuguang@ioz.ac.cn

Funding information
National Key Research and Development Program of China, Grant/Award Number: 2021YFC2301403 and 2022YFF0711000

Abstract

Background: This study aimed to construct and characterize a humanized influenza mouse model expressing hST6GAL1.

Methods: Humanized fragments, consisting of the endothelial cell-specific K18 promoter, human ST6GAL1-encoding gene, and luciferase gene, were microinjected into the fertilized eggs of mice. The manipulated embryos were transferred into the oviducts of pseudopregnant female mice. The offspring were identified using PCR. Mice exhibiting elevated expression of the hST6GAL1 gene were selectively bred for propagation, and in vivo analysis was performed for screening. Expression of the humanized gene was tested by performing immunohistochemical (IHC) analysis. Hematologic and biochemical analyses using the whole blood and serum of humanized hST6GAL1 mice were performed.

Results: Successful integration of the human ST6GAL1 gene into the mouse genome led to the overexpression of human SiaT ST6GAL1. Seven mice were identified as carrying copies of the humanized gene, and the in vivo analysis indicated that hST6GAL1 gene expression in positive mice mirrored influenza virus infection characteristics. The IHC results revealed that hST6GAL1 was expressed in the lungs of humanized mice. Moreover, the hematologic and biochemical parameters of the positive mice were within the normal range.

Conclusion: A humanized influenza mouse model expressing the hST6GAL1 gene was successfully established and characterized.

KEYWORDS
hST6GAL1, humanized mice, influenza animal model

1 | INTRODUCTION

Influenza virus infection is considered a global public health concern because of its pandemic potential, which has led to elevated morbidity and mortality rates worldwide.[1] These viruses frequently undergo genetic mutations, resulting in the emergence of new strains through antigenic shifts and drifts and unpredictable outbreaks of novel infectious diseases. Notable influenza pandemics include the 1918 Spanish H1N1, 1957 Asian H2N2, and 1968 Hong Kong H3N2 events, as well as the 2009 H1N1 pandemic, which was estimated to have caused 300 000 deaths within the first 12 months.[2] Additionally, seasonal influenza epidemics contribute to ≤650 000 deaths annually, causing a substantial economic burden.[3]

In the process of infecting the host with influenza virus, the receptor-binding characteristics of the hemagglutinin protein and the enzymatic activity of neuraminidase (NA) are pivotal determinants for viral replication in target host cells, particularly for different influenza viral subtypes.[4] The receptor-binding specificity of the hemagglutinin protein has a critical role in the cross-species transmission of influenza viruses. Hemagglutinin proteins from human influenza viruses typically prefer binding to sialic acids linked by α2,6 bonds, primarily found on the cell surfaces of human and other mammalian respiratory tracts. In contrast, hemagglutinin proteins from most avian influenza viruses tend to bind to sialic acids linked by α2,3 bonds.[5] Influenza viruses of subtype H1N1 and H3N2 can bind to α2,6 sialic acid receptors on host-cell surfaces, which are predominantly distributed in the upper-respiratory tract and ocular tissues of humans.[6] In contrast, the H5N1 influenza virus subtype can bind to α2,3 sialic acid receptors, mainly found in the upper-respiratory and digestive tracts of poultry.[7] Subtype H7N9 influenza virus can bind to both α2,3 sialic acid receptors and α2,6 sialic acid receptors, which are distributed in the upper-respiratory and digestive tracts of both poultry and humans.[8,9] Influenza type-B viruses also bind to α2,6 sialic acid receptors, similar to H1N1 and H3N2 subtypes.[10,11] In the influenza mouse model, BALB/c mice show increased expression of α2,3-linked sialic acid receptors in the lungs.[12] Therefore, commonly used BALB/c mice are more suitable for research involving avian influenza viruses that bind to α2,3 sialic acid receptors, whereas no optimal mouse model for human influenza viruses that bind to α2,6 sialic acid receptors has been established.

Regulation of the synthesis of α2,6 salivary acid receptors in the host is performed by the sialyltransferase (SiaT) family genes, fucosyltransferase (FUT) family genes, several transcription factors, signaling pathway factors, and regulatory proteins. The SiaT family genes encode SiaT proteins, which are key enzymes in sialic acid synthesis, that catalyze the transfer of sialic acid residues from donor molecules to substrate molecules, forming α2,6-linked sialic acid. SiaT family enzymes are capable of adding salivary acid residues at specific sites on cell-surface glycoproteins, which regulate the synthesis and specificity of the salivary acid receptor. The addition of fucose moieties to oligosaccharide or polysaccharide chains on glycoproteins to form fucose chains is primarily performed by the FUT family genes. Although these genes are not directly associated with salivary acid receptors, they indirectly affect its synthesis and function by regulating the structure and modification of the sugar chain. The ST6GAL1 gene, among the SiaT family genes, encodes an α2,6-linked sialic acid transferase responsible for transferring sialic acid to glucose residues of the sugar chain to form an α2,6-linked sialic acid structure. Moreover, the ST6GAL2 gene is important in the regulation of the synthesis of α2,6-linked salivate receptors. Although it is similar to ST6GAL1, it has a different substrate specificity and tissue-expression pattern and is involved in specific physiological processes. ST6GAL1 is typically expressed in various tissues, including the respiratory tract, liver, and intestines. In contrast, ST6GAL2 expression is relatively limited, primarily found in the nervous system, such as in embryonic- and adult-brain tissues, where it exhibits higher expression levels in neurons, glial cells, and some neuronal synapses.[13] Li et al. showed that the influenza virus grew to higher titers in Vero cells that overexpressed the ST6GAL1 gene than in those that did not.[14] Additionally, the adsorption of influenza virus particles on the cell surface was significantly reduced after silencing the ST6GAL1 gene in the airway epithelium.[15]

Consequently, in this study, the human ST6GAL1 gene was inserted into the mouse gene sequence, overexpressing and synthesizing the human α2,6-linked sialic acid receptors via human SiaT ST6GAL1, thereby constructing a humanized hST6GAL1 mouse model. This model is important for improving our understanding of the pathogenesis of influenza and advancing drug and vaccine development.

2 | MATERIALS AND METHODS

2.1 | Construction of the K18–hST6GAL1 plasmid

Standard molecular cloning techniques were used for the construction of a K18–hST6GAL1–luciferase plasmid.[16,17] The construction of the vector for transgenic mice overexpressing human α2,6-sialic acid receptors, K18–hST6GAL1, involves three components: K18, hST6GAL1, and luciferase. K18 serves as an endothelial cell-specific promoter,[18] hST6GAL1 represents the DNA sequence of human SiaT, and luciferase is a reporting system which uses luciferin as a substrate to detect firefly luciferase activities. The vector backbone used was PUC19L. Seamlessly linked components were used to construct the vector, designated as K18–hST6GAL1–luciferase–PUC19L. The K18 and luciferase plasmids were obtained from the Laboratory Animal Center of the Institute of Zoology, Chinese Academy of Sciences. The hST6GAL1 gene CDS sequence was retrieved from the NCBI website and synthesized by Shanghai Sangon Biotech Co., Ltd (Shanghai, China). The three gene segments were extensively amplified using polymerase chain reaction (PCR) and seamlessly connected to construct the K18–hST6GAL1–luciferase vector. Positive recombinant clones were identified using PCR. Moreover, k18-luc primers (F: acaagaggccttcctttggg; R: ttcgagtgggtagaatggcg) were used to perform

PCR amplification. Commercial kits (TransGen Biotech, Beijing, China; CU101; LabLead, MinElute 28 604, 50x) were used to perform the seamless ligation and gel-recovery steps. Additionally, the promoter–transgene junctions created by subcloning were sequenced to ensure that no sequence errors were introduced during the linker addition. An endotoxin-free plasmid purification kit (Tiangen, Beijing, China; DP118-02) was used to extract the plasmid, after which the plasmid was linearized through double digestion using SacI and SphI enzymes for microinjection.

2.2 | Animals

C57BL/6 mice were maintained by the Laboratory Animal Center of the Institute of Zoology, Chinese Academy of Sciences. The derived humanized mice were raised and bred at the same institution. The blood collection and dissection procedures were performed at the Laboratory Animal Center of the Chinese Center for Disease Control and Prevention. All experiments involving animals in this study were approved by the Laboratory Animal Welfare & Ethics Committee of the Institute of Zoology, Chinese Academy of Sciences, and the Chinese Center for Disease Control and Prevention.

2.3 | Generation of K18–hST6GAL1 humanized mice

The method described above was used to generate a linearized fragment of K18–hST6GAL1–luciferase. The linear DNA fragment was diluted to a concentration of 3–5 ng/μL in microinjection buffer. Fertilized oocytes were obtained from C57BL/6 female mice. The purification of the transgene, preparation of mice, microinjection into the fertilized C57BL/6 oocytes, and embryo implants were performed as described previously.[19–22] Briefly, pseudopregnant mice were prepared as embryo transfer recipients by mating females in natural estrus with vasectomized males. The females were ≥6–8 weeks of age and weighed 25–35 g. For experiments that required large numbers of preimplantation embryos, gonadotropins were often administered to females prior to mating to increase the number of oocytes that were ovulated by inducing superovulation. Pregnant mare's serum gonadotropin was used to mimic the oocyte maturation effect of the endogenous follicle-stimulating hormone, and human chorionic gonadotropin was used to mimic the ovulation-induction effect of luteinizing hormone. Pre-estrus C57BL/6 females of 3–4 weeks of age and weighing 12.5 g were subjected to super-exclusion and mated with normal males to form zygotes. The zygotes were captured and held in position by the holding capillary, and the injection pipette was carefully inserted into one of the pronuclei. DNA was injected until a clear swelling of the pronucleus was observed, and the injection pipette was then removed. The zygotes that survived microinjection were transferred the same day into the oviducts of 0.5-day pseudopregnant female mice.

2.4 | Genotype identification of K18–hST6GAL1 humanized mice

The humanized mice founders were identified using PCR. For this analysis, genomic DNA was extracted from the tails at 14–21 days of age and amplified using the following primers: K18-ST6F, 5′-cggtaccaataacagtaaaaggcagtacg-3′, and K18-ST6R, 5′-gataccaagcatcccagaggatgg-3′. The PCR amplification conditions were as follows: 98°C for 30 s, 98°C for 10 s, 68°C for 30 s (35 cycles), and 68°C for 7 min. The PCR products were loaded onto a 0.8% agarose gel and run at 120 V for 25 min. The gel was then visualized under ultraviolet light to observe the positions of the DNA bands.

2.5 | Assessing hST6GAL1 gene-expression intensity in mice

D-Fluorescein potassium salt solution (15 mg/mL) was prepared with sterile Dulbecco's phosphate-buffered saline (w/o Mg^{2+}, Ca^{2+}) and filtered through a 0.2-μm filter membrane for sterilization. An appropriate volume of 15-mg/mL luciferin solution was administered intraperitoneally to each mouse at a dose of 10 μL/g body weight. A small animal imaging system (Perkin Elmer, Greenville, SC, USA; IVIS® Lumina III) was used to perform subsequent imaging analysis approximately 10–15 min post-injection.

2.6 | Immunohistochemical analysis

Immunohistochemical analysis was performed as previously described.[23] After rehydration and antigen retrieval, 5-μm thin sections were blocked with 5% bovine serum albumin and then incubated with the primary antibody for 1 h and the corresponding secondary antibody for 1 h. The following primary antibodies were used: hST6GAL1 (bio-techne, Shanghai, China; AF5924). The secondary antibodies were: Horseradish peroxidase-labeled goat anti-rabbit immunoglobulin G (H + L) (ZSGB-BIO, Beijing, China; ZB-2301). For immunohistochemistry, a diaminobenzidine substrate kit was used to visualize staining that was examined using a Nikon microscope, and the images were captured using a Pannoramic DESK DW II (3DHISTECH Ltd, Budapest, Hungary).

2.7 | Hematologic physiological parameter analysis in K18–hST6GAL1 humanized mice

Blood samples were collected from the orbital sinus of F2 and subsequent generations of K18–hST6GAL1 humanized mice as well as C57BL/6 wild-type mice. The whole blood samples were analyzed for hematologic physiological parameters using the Mindray BC-5000VET hematology analyzer.

The reference values of hematologic physiological parameters were derived from C57BL/6 mice obtained from Charles River Laboratories (https://www.criver.com/resources/c57bl6-mouse-clinical-pathology-data).

2.8 | Blood biochemical parameter analysis in K18–hST6GAL1 humanized mice

Following blood collection from the orbital sinus of F2 and subsequent generations of K18–hST6GAL1 humanized mice, as well as C57BL/6 wild-type mice, serum was obtained by centrifugation. The Mindray BS-240VET blood biochemical analyzer, with kits from the same commercial company, were used to perform the biochemical analyses in the serum. The reference values of the blood biochemical parameters were derived from a study by Boehm et al.[24]

2.9 | Statistical analysis

SPSS 25.0 was used to perform the statistical analyses, including normality and variance tests, for each group. The normally distributed data were presented as mean ± standard deviation. Student's *t*-test was performed to compare means between the two groups. Statistical significance was accepted for values of $p < 0.05$.

3 | RESULTS

3.1 | Construction of K18–hST6GAL1 expression vectors

The K18–hST6GAL1 expression vector comprises the epithelial cell K18 promoter, coding sequence (CDS) of the human ST6GAL1 gene, luciferase, and PUC19L vector (Figure 1A). After extensive amplification of K18, hST6GAL1, luciferase sequences, and PUC19L vector, seamless ligation was performed to assemble the vector. PCR was performed on the resulting positive recombinant clones, with the target band observed at 1773 bp (Figure 1B). The electrophoresis results revealed that the clones were positive except for clones #12, #14, #22, #26, #29, #30, #34, #36, #38, #41, and #46, which tested negative. Of the positive clones, #2, #23, and #24 were randomly chosen for sequencing. Following the purification using endotoxin-free purification methods of correctly sequenced plasmids (Figure 1C), they were robustly amplified for subsequent enzyme digestion and microinjection. The validated K18–hST6GAL1 recombinant plasmid underwent linearization

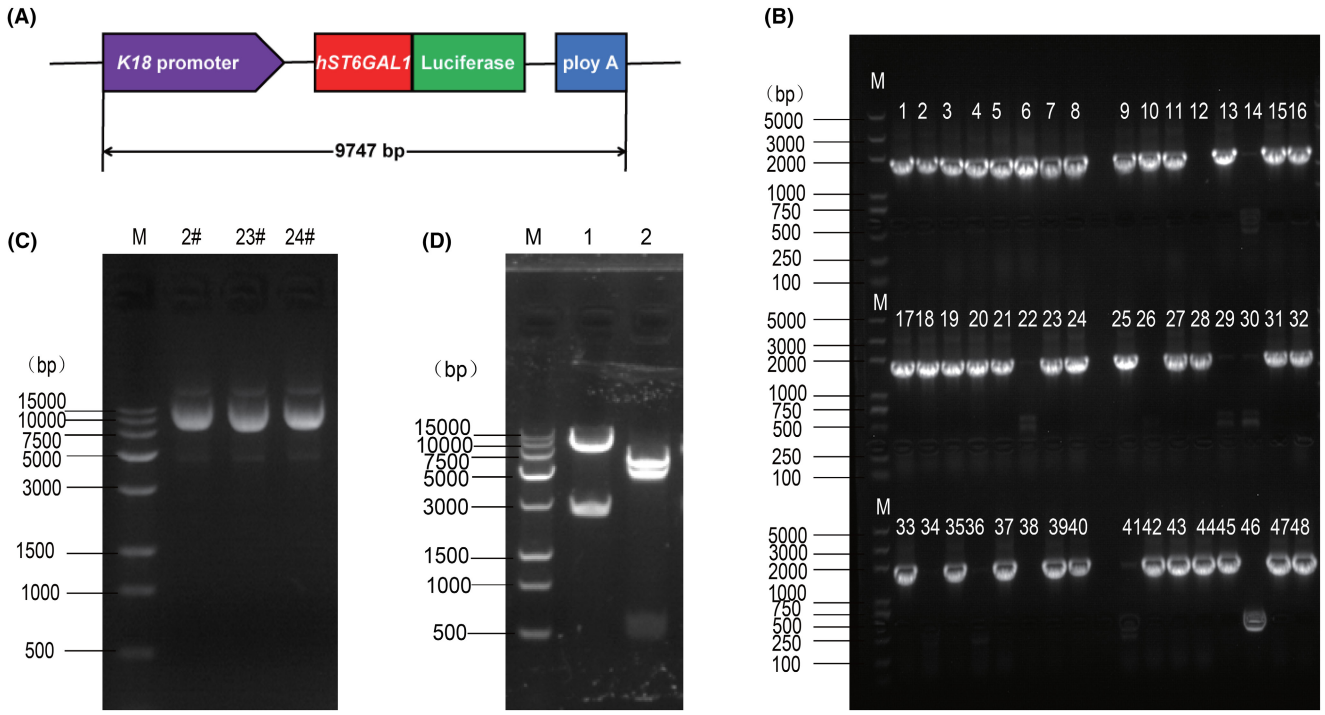

FIGURE 1 Construction of the K18–hST6GAL1 expression vector. (A) Schematic representation of the construction of the K18–hST6GAL1 expression vector. The components included promoter of K18, coding sequence of the human ST6GAL1 gene (CDS), luciferase, and PUC19L vector. (B) Results of the PCR and electrophoresis identification of positive clones of the K18–hST6GAL1 recombinant plasmid. M, DNA 2 k Plus marker (Trans2k Plus BM111), 1–48. Randomly selected 48 clones; target band size, 1773 bp. (C) PCR and electrophoresis identification of the K18–hST6GAL1 recombinant plasmid before enzyme digestion and linearization. M, DNA 15 K marker (Trans15K BM161) (from left to right, K18-hST6GAL1 recombinant plasmids #2, #23, and #24). The target band for the positive recombinant plasmids is 9747 bp, and the electrophoresis results indicated correct banding. (D) Gel electrophoresis of the DNA recovered after SacI + SphI double-enzyme digestion of the K18–hST6GAL1 expression vector. M, DNA 15 K marker (Trans15K BM161); 1, two fragments after SacI+SphI double-enzyme digestion, with band sizes matching expectations; 2, K18-hst6-23# plasmid before enzyme digestion.

through SacI and SphI double-enzyme digestion (Figure 1D), with the gel-extracted large fragment of 7100 bp used for microinjection.

3.2 | Appearance of the K18–hST6GAL1 humanized mice founders

In accordance with the aforementioned procedures, the linearized DNA fragments of purified K18–hST6GAL1 and prokaryotic microinjection were used to generate humanized mice. A total of 20 mice were obtained, exhibiting the appearance shown in Figure 2. The K18–hST6GAL1 humanized mice showed no differences from C57BL/6 mice at ages 3, 5, 10, and 21 days.

3.3 | Genotyping of K18–hST6GAL1 humanized mice founders

Based on the above procedures, 20 founder humanized mice were generated via pronuclear microinjection of purified linearized K18–hST6GAL1 DNA fragments. PCR identification was performed on the obtained F0-generation mice, revealing seven positive humanized mice classified as #4, #8, #12, #14, #15, #17, and #20 (Figure 3).

3.4 | In vivo analysis of K18–hST6GAL1 humanized mice founders

The human ST6GAL1 gene and the luciferase gene are specifically coexpressed in the humanized mice. In vivo imaging of luciferase can be used to determine the expression sites and levels of the human ST6GAL1 gene. The seven mice with positive genotypic identification (#4, #8, #12, #14, #15, #17, and #20) were subjected to in vivo analysis to assess gene-expression intensity. The results showed that the hST6GAL1 gene-expression levels were increased in the respiratory system, including the lungs and trachea, making these mice suitable for influenza research. Among them, F014# and F017# mice exhibited higher expression levels (Figure 4).

FIGURE 2 External characteristics of the K18–hST6GAL1 humanized mice founders. (A–D) represent the K18-hST6GAL1 humanized mice at ages 3, 5, 10, and 21 days.

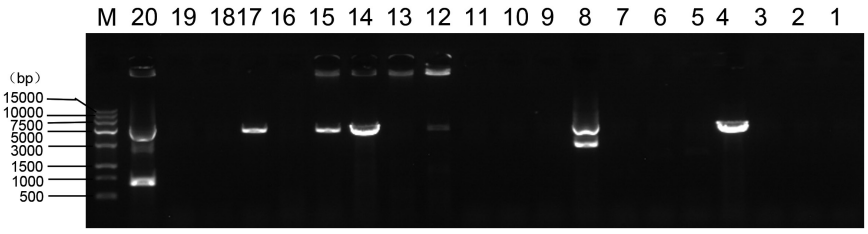

FIGURE 3 Genotypic identification results of K18–hST6GAL1 humanized mice founders. Genotypic identification results of the K18–hST6GAL1 humanized mice (F0 generation). M, DNA marker, Trans15K BM161; #1–20 represent the 20 individual offspring. Among them, F0-4, −8, −12, −14, −15, −17, and − 20 were identified as humanized positive mice.

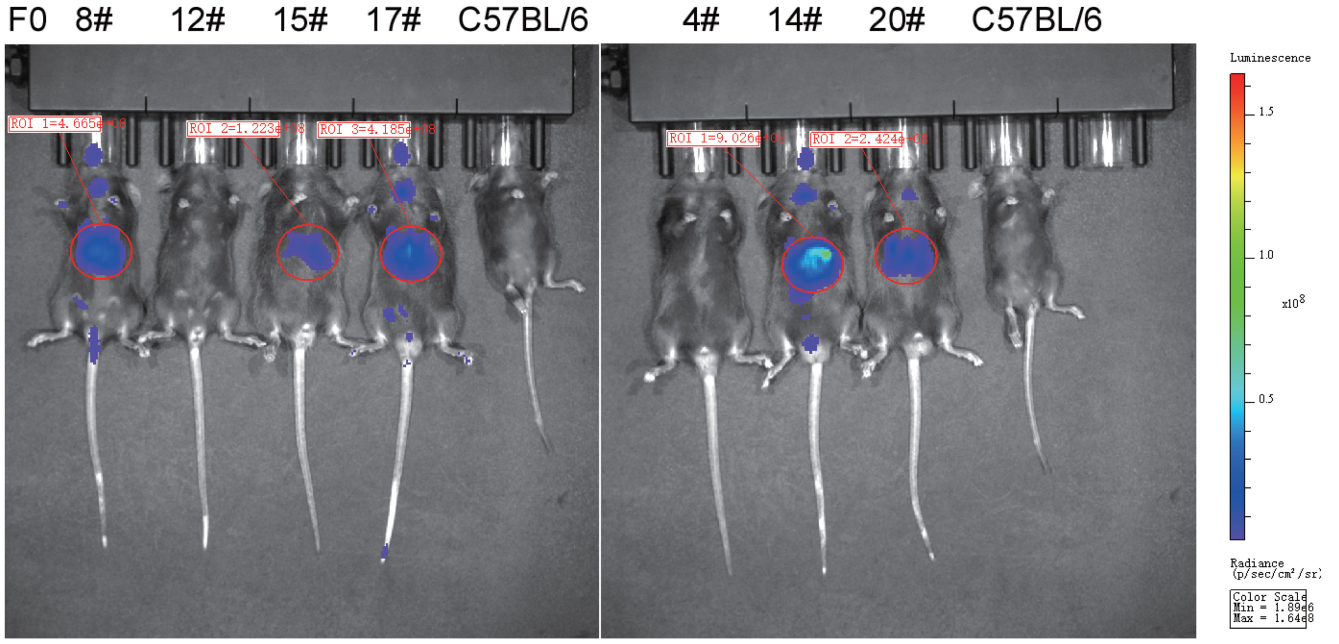

FIGURE 4 In vivo analysis results of K18–hST6GAL1 humanized mice founders. In vivo analysis results of the K18–hST6GAL1 humanized mice F0 generation. Control group, C57BL/6; experimental group, F0-4, −8, −12, −14, −15, −17, and −20 mice with positive genotypic identification. After the comparison, #14 and #17 founder mice were selected for breeding.

3.5 | Breeding of K18–hST6GAL1 humanized mice

#F014 and #F017 positive transgenic founder mice were selected for mating with C57BL/6 wild-type mice, yielding the F1 generation. Genotypic identification and in vivo analysis were performed on F1 mice, and those identified as positive in both aspects were further mated with C57BL/6 wild-type mice to obtain the F2 generation. For subsequent generations (F2 and beyond), the mice with positive genotypic identification and in vivo analysis were selectively bred to establish a stable humanized hST6GAL11 mouse model for further research (Figure 5).

3.6 | Immunohistochemistry analysis

Immunohistochemistry showed that hST6GAL1 was not expressed in the lungs of C57BL/6 (Figure 6A). However, hST6GAL1 was expressed in the lungs of K18–hST6GAL1 humanized mice. Specifically, it was mainly expressed in the pseudostratified ciliated columnar epithelium or simple ciliated columnar epithelium of the bronchioles, with a reduced expression level in alveolar type II epithelial cells (Figure 6B).

3.7 | Blood physiological indexes in K18–hST6GAL1 humanized mice

A total of 16 hematologic parameters were measured, including white blood cell count (WBC), neutrophils (Neu), lymphocytes (Lym), monocytes (Mon), percentage of neutrophils (Neu%), percentage of lymphocytes (Lym%), percentage of monocytes (Mon%), red blood cell count (RBC), hemoglobin (HGB), hematocrit (HCT), mean corpuscular volume (MCV), mean corpuscular hemoglobin concentration (MCH), mean corpuscular hemoglobin (MCHC), red-cell distribution width (RDW-CV), platelet count (PLT), and mean platelet volume (MPV).

The blood physiological parameters of K18–hST6GAL1 humanized mice and C57BL/6 wild-type mice were within the normal range. Comparison of K18–hST6GAL1 humanized mice with C57BL/6 wild-type mice showed significant differences ($p < 0.05$) in seven parameters related to lymphocytes. The remaining 15 parameters showed no significant differences ($p > 0.05$) (Table 1). The higher lymphocyte count in K18–hST6GAL1 humanized mice than in C57BL/6 wild-type mice indicated that K18–hST6GAL1 humanized mice may be more sensitive to pathogenic infections.

3.8 | Hematologic biochemical indexes of K18–hST6GAL1 humanized mice

A total of nine blood biochemical parameters were assessed, including alanine aminotransferase (ALT), aspartate aminotransferase (AST), total protein (TP), α-Amylase (α-AMY), creatinine (CREA-S), blood urea nitrogen (UREA), glucose (Glu-G), total cholesterol (TC), and triglycerides (TG). The blood biochemical parameters of K18–hST6GAL1 humanized mice and C57BL/6 wild-type mice were within the normal range. When compared with C57BL/6 wild-type mice, the K18–hST6GAL1 humanized mice showed no significant differences ($p > 0.05$) in the nine parameters (Table 2).

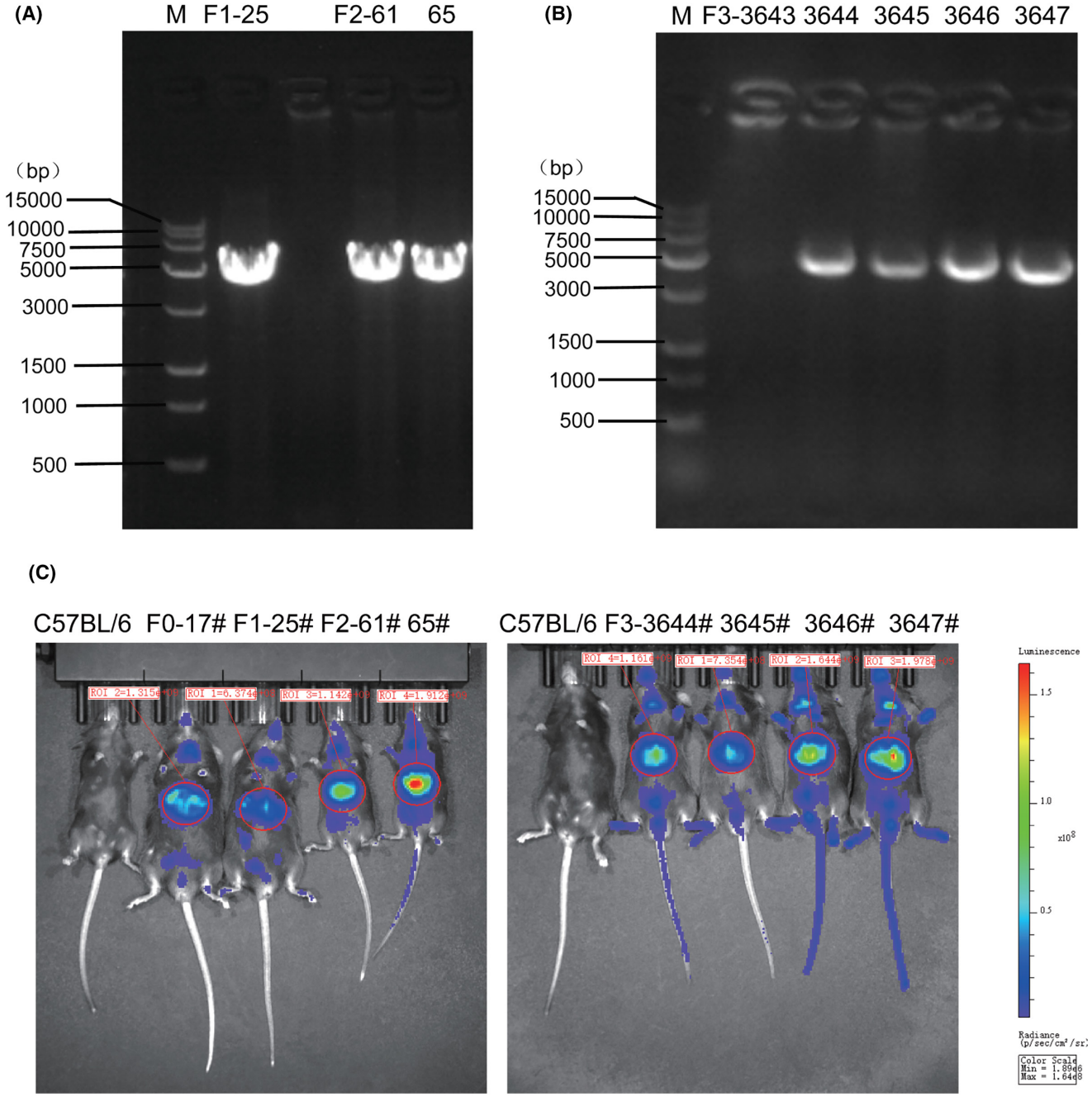

FIGURE 5 Breeding of K18–hST6GAL1 humanized mice. (A) Genotypic identification results of K18–hST6GAL1 humanized mice F1 (F2 generation). M, DNA marker, Trans15K BM161; F1-25 and F2-61 and −65 were identified as positive genotypes. (B) Genotypic identification results of K18-hST6GAL1 humanized mice F3 generation. M, DNA marker, Trans15K BM161; F3-3643 identified as negative and F3-3644, −3645, −3646, and −3647 identified as positive. (C) In vivo analysis results of the K18–hST6GAL1 humanized mice (F1, F2, and F3 generations). Control group, C57BL/6; experimental group, F1-25, F2-61, and −65 and F3-3644, −3645, −3646, and −3647 mice with positive genotypic identification.

4 | DISCUSSION

Currently, mice, ferrets, guinea pigs, and nonhuman primates are the prominent animal models in the field of influenza research. While mice lack the natural receptivity to human influenza viruses, necessitating adaptation through multiple pulmonary passages, their use as an influenza model is grounded in the application of mouse-adapted strains, such as PR8 and X-31.[25] Despite not being an ideal transmission model, mice offer advantages, such as rapid reproduction, ease of handling, low cost, genetic clarity, and well-established immune reagents. Ferrets, which have similarities in pulmonary pathology and cell receptors to humans,[26] are favored for studying influenza virus pathogenicity and transmissibility.[27] However, their limitations include the lack of specific reagents for analyzing infection

and immune responses, high experimental costs, and challenges in care and manipulation. Guinea pigs, occasionally used for influenza research, share physiological similarities with humans but present challenges in the study of pathogenesis because of the absence of clinical symptoms postinfection and specific reagents.[28] Moreover, nonhuman primates, which are closely related to humans, serve as valuable models for influenza pathogenesis and vaccine/drug efficacy evaluation. However, ethical constraints, high costs, complex housing conditions, and specialized personnel requirements limit their widespread use in influenza research.

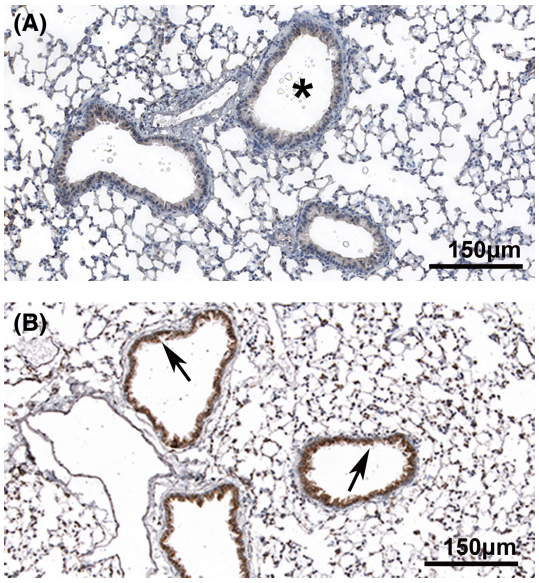

FIGURE 6 Immunohistochemistry analysis of Hst6GAL1 protein expression in the lungs of wild-type and K18–Hst6GAL1 humanized mice. (A) hST6GAL1 protein expression in the lungs of C57BL/6 (asterisks). (B) hST6GAL1 protein expression in the lungs of K18–hST6GAL1 humanized mice (arrows).

Humanized mice represent mouse models incorporating functional human genes, cells, or tissues. Typically achieved through transgenic or homologous recombination methods, the introduction of human genes into mice allows the manifestation of diseases with pathological, physiological, and immune responses mirroring those in humans. Consequently, humanized mouse models have shown extensive applications in various research fields, including infectious diseases, cancer, and hematologic disorders. For example, uPA-SCID mice and TK-NOG mice are commonly used in hepatitis B virus studies,[29] whereas humanized CSF-1R gene knock-in mice serve as valuable models for evaluating the efficacy of tumor immunotherapy antibodies and screening-targeted anti-tumor drugs. In influenza research, some humanized immunodeficient mice are used for influenza vaccine studies.[30,31] However, only a few models involving influenza-susceptible mice constructed through the humanization of sialic acid receptors have been reported.

When using humanized mice for vector construction, the first consideration after identifying the exogenous genes to be expressed is the selection of appropriate promoters and regulatory elements. This ensures the appropriate expression pattern of the exogenous DNA in the mouse. Promoters commonly used in the study of respiratory diseases include the CMV promoter, which produces high levels of transcriptional activity in most mammalian cells;[32] the calcitonin gene-related peptide promoter, which is expressed in neurons and epithelial cells

TABLE 1 Comparison of blood physiological parameters between K18–hST6GAL1 humanized mice and C57BL/6 wild-type mice ($n=3$).

Blood physiological indexes	K18-hST6GAL1	C57BL/6	95% Interval	
			Low	High
WBC ($\times10^9$/L)	7.56±1.36	6.9±1.05	3.90	13.94
Neu ($\times10^9$/L)	0.82±0.13	0.66±0.39	0.42	2.55
Lym ($\times10^9$/L)	5.47±2*	4.59±0.39*	2.88	10.92
Mon ($\times10^9$/L)	0.31±0.05	0.21±0.06	0.17	0.69
Neu (%)	11.03±2.48	9.2±4.69	7.44	22.67
Lym (%)	70.93±13	67.07±6.71	70.19	87.82
Mon (%)	4.33±1.36	3.07±1.07	2.19	7.06
RBC ($\times10^{12}$/L)	11.24±1.31	11.68±0.36	7.14	12.20
HGB (g/L)	186.33±27.57	218±9	10.80	19.20
HCT (%)	52.23±9.78	53.73±1.32	37.30	62.00
MCV (fL)	46.2±3.22	46.03±0.93	42.70	56.00
MCH (pg)	16.6±1.47	18.67±0.21	11.70	16.30
MCHC (g/L)	360±46.36	404.67±12.5	24.60	34.90
RDW-CV (%)	16.1±1.61	14.77±0.4	15.90	20.30
PLT ($\times10^9$/L)	1076±97.75	1142.33±115.63	841.00	2159.00
MPV (fL)	5.83±0.15	6±0.53	4.30	6.10

*$p<0.05$.

TABLE 2 Comparison of blood biochemical parameters between K18–hST6GAL1 humanized mice and C57BL/6 wild-type mice ($n = 3$).

Blood biochemical indices	K18–hST6GAL1	C57BL/6	95% Interval	
			Low	High
ALT (U/L)	38.77 ± 1.33	36.23 ± 14.12	13.00	43.00
AST (U/L)	76.07 ± 13.49	99.33 ± 30.39	12.00	89.00
TP (g/L)	59 ± 2.5	58.47 ± 1.4	3.00	5.00
α-AMY (U/L)	2600.7 ± 206.86	2217.73 ± 285.84	1197.00	2722.00
CREA-S (μmol/L)	7.43 ± 3.1	13.87 ± 4.54	11.00	28.00
UREA (mmol/L)	8.38 ± 1.93	7.04 ± 1.13	6.00	11.50
Glu-G (mmol/L)	8.8 ± 1.12	7.46 ± 2.74	5.90	16.70
TG (mmol/L)	0.76 ± 0.06	1.26 ± 0.07	0.70	1.90
TC (mmol/L)	2.06 ± 0.3	1.21 ± 0.08	1.10	2.60

and is often used to study neuron-related respiratory disorders;[33] and the K18 promoter, which is used in the construction of respiratory viral animal models because of its high activity and specificity in epithelial cells. In this experiment, which targeted the human ST6GAL1 gene, we successfully constructed a K18 endothelial cell-specific promoter-driven hST6GAL1 gene-targeting vector. We used microinjection technology to establish humanized mice with a high expression of human ST6GAL1. From the group of seven founder humanized mice, three mice with relatively high expression levels were selected to mate with wild-type C57BL/6 mice, generating the F1 generation of humanized mice. Moreover, genotype identification and in vivo imaging analysis were conducted on the F1-generation mice, and those with positive genotype identification and positive in vivo imaging were selected to mate with wild-type C57BL/6 mice, which produced the F2 generation. Genotype identification and in vivo imaging analysis of the F2 generation and subsequent generations of mice showed the successful insertion of the hST6GAL1 gene into the mouse genome and its expression consistent with the infection characteristics of the influenza virus.

Hematologic and biochemical parameters in experimental animals are pivotal indicators in biomedical research, serving as benchmarks to evaluate animal health and select suitable subjects. These parameters have critical roles in various research disciplines, including pathology and toxicology, and are governed by a combination of intrinsic genetic factors and external environmental influences. Genetic factors provide the underlying basis for determining these parameters, whereas environmental factors act as external conditions influencing variations in the hematologic and biochemical parameters. In this study, hematologic and biochemical analyses were performed on the whole blood and serum of the hST6GAL1-positive mice. The results showed that there were no significant differences in the majority of hematologic and biochemical parameters between the wild-type mice and humanized hST6GAL1 mice. This finding indicates that the overall hematologic and biochemical profiles of humanized hST6GAL1 mice were within the normal range.

In this investigation, we have successfully established and characterized a humanized influenza mouse model expressing the hST6GAL1 gene. This model serves as a promising platform for direct infection with human influenza viruses, eliminating the need for an adaptation process within the mouse host. The humanized mouse model effectively mirrors the clinical features of influenza, providing opportunities to investigate the mechanisms of influenza pathogenesis, validate new drug targets, and assess the efficacy of drugs and vaccines.

5 | CONCLUSIONS

In conclusion, a humanized influenza mouse model expressing the hST6GAL1 gene was successfully established and characterized.

AUTHOR CONTRIBUTIONS

Lyu Chao: Conceptualization, Methodology, Data curation, Investigation, Validation, Writing—Original draft, Review & Editing. **Han Feng**, **Gao Qian**, **Lv Limin**: Methodology, Data curation, Investigation, Validation. **Lu Ziwei**, **Lu Shuangshuang**, **Li Xiaoyan**, **Hu Yuechao**, **Yang Mengjie**, **Zhao Yingze**: Methodology, Data curation. **Duo Shuguang**, **Liu Jun**: Conceptualization, Methodology, Data curation, Investigation, Validation, Writing—Review & Editing. **Lu Xuancheng**: Conceptualization, Methodology, Data curation, Investigation, Validation, Writing—Original draft, Review & Editing.

ACKNOWLEDGMENTS

We appreciate the staff of the Laboratory Animal Center of the Institute of Zoology, Chinese Academy of Sciences and the Laboratory Animal Center of the Chinese Center for Disease Control and Prevention.

FUNDING INFORMATION

This work was supported by grants from the National Key Research and Development Program of China (2021YFC2301403 and 2022YFF0711000).

CONFLICT OF INTEREST STATEMENT

The authors declare that they have no conflict of interest.

ETHICS STATEMENT

All experiments involving animals of this study were approved by the Laboratory Animal Welfare & Ethics Committee of the Institute of Zoology, Chinese Academy of Sciences, and the Chinese Center for Disease Control and Prevention.

ORCID

Lyu Chao https://orcid.org/0009-0003-3569-9544
Lu Shuangshuang https://orcid.org/0000-0002-5969-9421

REFERENCES

1. Glezen WP. Emerging infections: pandemic influenza. *Epidemiol Rev*. 1996;18(1):64-76.
2. Dawood FS, Iuliano AD, Reed C, et al. Estimated global mortality associated with the first 12 months of 2009 pandemic influenza a H1N1 virus circulation: a modelling study. *Lancet Infect Dis*. 2012;12(9):687-695.
3. Organization, W.H. Influenza (Seasonal). 2023. Available from https://www.who.int/news-room/fact-sheets/detail/influenza-(seasonal)
4. Liu WJ, Wu Y, Bi Y, et al. Emerging HxNy Influenza A Viruses. *Cold Spring Harb Perspect Med*. 2022;12(2):a038406.
5. Nelli RK, Kuchipudi SV, White GA, Perez BB, Dunham SP, Chang KC. Comparative distribution of human and avian type sialic acid influenza receptors in the pig. *BMC Vet Res*. 2010;6:4.
6. Nicholls JM, Bourne AJ, Chen H, Guan Y, Peiris JSM. Sialic acid receptor detection in the human respiratory tract: evidence for widespread distribution of potential binding sites for human and avian influenza viruses. *Respir Res*. 2007;8(1):73.
7. Abdelwhab EM, Hafez HM. An overview of the epidemic of highly pathogenic H5N1 avian influenza virus in Egypt: epidemiology and control challenges. *Epidemiol Infect*. 2011;139(5):647-657.
8. Murray J, Martin DE, Hosking S, Orr-Burks N, Hogan RJ, Tripp RA. Probenecid inhibits influenza A(H5N1) and A(H7N9) viruses in vitro and in mice. *Viruses*. 2024;16(1):152.
9. Lei Y, Sun Y, Wu W, et al. Influenza H7N9 virus disrupts the monolayer human brain microvascular endothelial cells barrier in vitro. *Virol J*. 2023;20(1):219.
10. Wilson JL, Akin E, Zhou R, et al. The influenza B virus victoria and yamagata lineages display distinct cell tropism and infection induced host gene expression in human nasal epithelial cell cultures. *Viruses*. 2023;15(9):1956.
11. Rosu ME, Lexmond P, Bestebroer TM, et al. Substitutions near the HA receptor binding site explain the origin and major antigenic change of the B/Victoria and B/Yamagata lineages. *Proc Natl Acad Sci USA*. 2022;119(42):e2211616119.
12. Ibricevic A, Pekosz A, Walter MJ, et al. Influenza virus receptor specificity and cell tropism in mouse and human airway epithelial cells. *J Virol*. 2006;80(15):7469-7480.
13. Lehoux S, Groux-Degroote S, Cazet A, et al. Transcriptional regulation of the human ST6GAL2 gene in cerebral cortex and neuronal cells. *Glycoconj J*. 2010;27(1):99-114.
14. Li N, Qi Y, Zhang FY, et al. Overexpression of alpha-2,6 sialyltransferase stimulates propagation of human influenza viruses in Vero cells. *Acta Virol*. 2011;55(2):147-153.
15. Wu D, Huang W, Wang Y, et al. Gene silencing of β-galactosamide α-2,6-sialyltransferase 1 inhibits human influenza virus infection of airway epithelial cells. *BMC Microbiol*. 2014;14:78.
16. Sambrook J, Fritsch EF, Maniatis T. *Molecular cloning: a laboratory manual*. Cold spring harbor laboratory press; 1989.
17. Ausubel FM et al. Short protocols in molecular biology. *N Y*. 1992;275:28764-28773.
18. Chow YH, O'Brodovich H, Plumb J, et al. Development of an epithelium-specific expression cassette with human DNA regulatory elements for transgene expression in lung airways. *Proc Natl Acad Sci USA*. 1997;94(26):14695-14700.
19. Rall GF, Mucke L, Oldstone MB. Consequences of cytotoxic T lymphocyte interaction with major histocompatibility complex class I-expressing neurons in vivo. *J Exp Med*. 1995;182(5):1201-1212.
20. Hogan B, Constantini F, Lacy E. *Manipulating the Mouse Genome*. Cold Spring Harbor Laboratory Press; 1986.
21. Mucke L, Oldstone MB, Morris JC, Nerenberg MI. Rapid activation of astrocyte-specific expression of GFAP-lacZ transgene by focal injury. *New Biol*. 1991;3(5):465-474.
22. Oldstone MB, Nerenberg M, Southern P, Price J, Lewicki H. Virus infection triggers insulin-dependent diabetes mellitus in a transgenic model: role of anti-self (virus) immune response. *Cell*. 1991;65(2):319-331.
23. Chen M, Li S, Liu S, et al. Infection of SARS-CoV-2 causes severe pathological changes in mouse testis. *J Genet Genomics*. 2023;50(2):99-107.
24. Boehm O, Zur B, Koch A, et al. Clinical chemistry reference database for Wistar rats and C57/BL6 mice. *Biol Chem*. 2007;388(5):547-554.
25. Palani S, Uddin MB, McKelvey M, Shao S, Sun K. Immune predisposition drives susceptibility to pneumococcal pneumonia after mild influenza a virus infection in mice. *Front Immunol*. 2023;14:1272920.
26. Jayaraman A, Chandrasekaran A, Viswanathan K, Raman R, Fox JG, Sasisekharan R. Decoding the distribution of glycan receptors for human-adapted influenza a viruses in ferret respiratory tract. *PLoS One*. 2012;7(2):e27517.
27. Belser JA, Eckert AM, Tumpey TM, Maines TR. Complexities in ferret influenza virus pathogenesis and transmission models. *Microbiol Mol Biol Rev*. 2016;80(3):733-744.
28. Canning BJ, Chou Y. Using Guinea pigs in studies relevant to asthma and COPD. *Pulm Pharmacol Ther*. 2008;21(5):702-720.
29. Lai F, Wee CYY, Chen Q. Establishment of humanized mice for the study of HBV. *Front Immunol*. 2021;12:638447.
30. Yu CI, Gallegos M, Marches F, et al. Broad influenza-specific CD8+ T-cell responses in humanized mice vaccinated with influenza virus vaccines. *Blood*. 2008;112(9):3671-3678.
31. Wada Y, Nithichanon A, Nobusawa E, et al. A humanized mouse model identifies key amino acids for low immunogenicity of H7N9 vaccines. *Sci Rep*. 2017;7(1):1283.
32. Wang M, Hou S, Lu X, Li J, Li R, Yan X. Interleukin-37 inhibits inflammation activation and disease severity of PM2.5-induced airway hyperresponsiveness. *Ecotoxicol Environ Saf*. 2021;227:112890.
33. Perl AK et al. Conditional recombination reveals distinct subsets of epithelial cells in trachea, bronchi, and alveoli. *Am J Respir Cell Mol Biol*. 2005;33(5):455-462.

How to cite this article: Chao L, Feng H, Qian G, et al. Establishment of a humanized ST6GAL1 mouse model for influenza research. *Anim Models Exp Med*. 2024;7:337-346. doi:10.1002/ame2.12449